Spinodal equation of state for rutile TiO_2

E. Francisco,[1] M. Bermejo,[2] V. García Baonza,[3] L. Gerward,[4] and J. M. Recio[1]
[1]*Departamento de Química Física y Analítica, Universidad de Oviedo, E-33006 Oviedo, Spain*
[2]*Departamento de Física, Universidad de Oviedo, E-33007 Oviedo, Spain*
[3]*Departamento de Química Física, Universidad Complutense de Madrid, E-28040 Madrid, Spain*
[4]*Department of Physics, Technical University of Denmark, DK-2800 Lyngby, Denmark*
(Received 2 October 2002; published 28 February 2003)

We present a general computational scheme to extend the spinodal equation of state [García Baonza *et al.*, Phys. Rev. B **51**, 28 (1995)] to the interpretation of the cell parameters response to hydrostatic pressure in orthogonal lattices. As an important example, we analyze the pressure (p)–volume (V)–temperature (T) data of the rutile phase of TiO_2. We show that results of *ab initio* perturbed ion calculations and very recent x-ray-diffraction experiments of isothermal compression on this system closely follow the spinodal conduct. The computational scheme permits the incorporation of temperature effects in the static calculation as well as in the room-temperature experimental data. Overall, we find highly consistent results and good theory-experiment agreement for a significant series of observables, including structural parameters, $p-V$ diagram, bulk modulus, linear compressibilities, and thermal-expansion coefficient. The observed discrepancies in the pressure first derivative of the bulk modulus can be traced back to the difference between the theoretical and the experimental spinodal pressure.

DOI: 10.1103/PhysRevB.67.064110 PACS number(s): 64.30.+t, 62.50.+p, 65.40.−b, 61.50.Ah

I. INTRODUCTION

The pressure (p)–volume (V)–temperature (T) equation of state (EOS) is a fundamental equation in many areas of basic and applied condensed-matter research. The pressure response of the structural parameters and the phase sequences induced by hydrostatic pressure in crystalline materials have been among the topics more extensively studied in the last decade. This trend has been fueled by developments in instrumentation and improvements in the experimental techniques that now allow the accurate characterization of polymorphs at different conditions of pressure and temperature.[1]

The fresh flow of $p-V-T$ data has stimulated the theoretical analysis. In this line, García Baonza *et al.*[2] have recently proposed and discussed a different EOS based on the so-called pseudospinodal hypothesis. This spinodal equation of state (SEOS) has been proved to be valid for a variety of solids and liquids up to several Mbar. Its most remarkable feature is the power-law pressure dependence of the bulk modulus B_T given by a divergence exponent γ. It has been confirmed that this exponent takes a universal value of 0.85, not only for crystalline solids, but also for liquids, polymers, molten salts, or liquid metals.[2,3] This is an attractive feature of the SEOS approach because it can be applied to systems undergoing phase transitions. Originally the SEOS was derived as a simple and efficient fitting tool, but a series of high-pressure studies has revealed its multipurpose usefulness and theoretical relevance.[4,5]

Since temperature effects can be easily incorporated in the SEOS through a simple Mie-Grüneisen model, this equation becomes a complete EOS containing five characteristic parameters.[4,5] Among the useful properties of this equation we recall here that (i) its temperature dependence is given by the temperature dependence of the spinodal pressure, and (ii) its five parameters can be determined either theoretically or using a single experiment at a given reference temperature, in contrast to other models found in the literature.[6] It is also important to emphasize that the isothermal SEOS can be easily reorganized to express the pressure as an explicit function of the volume, or vice versa. All these distinctive features make this equation of state specially adequate for our purposes.

The main objective of this work is to show that the SEOS can be easily extended to describe the behavior of linear structural parameters with pressure in orthogonal lattices. A second objective is to analyze the performance of the SEOS in the description of the high-p and high-T data of TiO_2. The stable phase of this material at normal conditions, rutile, has, among many others, the interesting property of being a crystallographic analog of stishovite SiO_2, a significant high-pressure quartz phase in the Earth's lower mantle.[7] The structural and elastic behavior of rutile TiO_2 at several p and T conditions has been recently investigated theoretically[8–12] and experimentally.[7,13,14] The theoretical bulk modulus at zero pressure (B_0) lies in the range 200–240 GPa and its first pressure derivative at zero pressure (B_0') between 4 and 6. The experimental data show narrower ranges: B_0 values cluster around 210 GPa and B_0' around 6.7, although this high value should be taken with caution.[15] The temperature dependence of the volumetric thermal-expansion coefficient $\alpha_v(T)$ is known also with some ambiguity since Toulokian *et al.*[16] and Saxena *et al.*[17] report two different sets of values. Furthermore, the c/a ratio of the rutile tetragonal unit cell does not follow the so-called inverse relationship,[18] since it increases with pressure and temperature.

Our work is organized in three separate goals: (i) to develop and discuss a general strategy for describing $p-T-V$ data with the SEOS, as well as $p-T-a$ data with the so-called linear SEOS, where a is any unit-cell parameter; (ii) to report theoretical results on the pressure and tempera-

ture response of the volume and lattice parameters of the rutile TiO_2; and (iii) to examine the consistency of the SEOS in the description of structural, thermal, and elastic properties obtained from our theoretical calculations and several experimental sources.

The layout of the paper is the following. Section II, with three subsections, contains the details of the proposed fitting procedure for the isothermal $p-V$ and $p-a$ data as well as the temperature dependence of the SEOS. In Sec. III we present our theoretical results and the discussion of the isothermal $p-V$ data and the thermal response. The main conclusions are collected at the end of the paper.

II. SPINODAL EQUATION OF STATE

A. Fitting scheme

The universal isothermal SEOS is given by the expression[4,5]

$$V(p)=V_{\mathrm{sp}}\exp\left\{-\frac{K^*}{(1-\gamma)}[p-p_{\mathrm{sp}}]^{1-\gamma}\right\}, \tag{1}$$

where K^* is an amplitude, and the spinodal volume V_{sp} and the spinodal pressure p_{sp} are the volume and divergence pressure along the pseudospinodal curve, respectively. They are related to the more familiar quantities V_0, B_0, and B_0', by the equations

$$B_0=\frac{[-p_{\mathrm{sp}}]^{\gamma}}{K^*}, \tag{2}$$

$$B_0'=\frac{\gamma B_0}{[-p_{\mathrm{sp}}]}, \tag{3}$$

and

$$V_0=V_{\mathrm{sp}}\exp\left[\frac{\gamma}{(\gamma-1)B_0'}\right]. \tag{4}$$

The exponent γ is a universal parameter of the SEOS that takes a fixed value of 0.85 which is strongly supported by both previous[4,5] and recent results.[3] Moreover, a detailed numerical analysis of this parameter shows that it deviates from 0.85 in less than 3% for a variety of substances in different phases. Thus the isothermal SEOS becomes a two-parameter EOS, since K^*, V_{sp}, and p_{sp} can be evaluated from B_0 and B_0' provided the zero-pressure volume V_0 is known.

The usual fitting procedure has been to use a Levengerg-Marquard routine (usually implemented in commercial packages) to obtain the characteristic parameters. However, a simpler and more robust procedure may be performed by noting that the SEOS can be linearized in the form

$$\ln\left(\frac{V}{V_0}\right)=y=M(1-x), \tag{5}$$

where

$$x=\left[1+\frac{p}{(-p_{\mathrm{sp}})}\right]^{1-\gamma}=\left[1+\frac{B_0'}{\gamma B_0}p\right]^{1-\gamma}, \tag{6}$$

and

$$M=\frac{K^*(-p_{\mathrm{sp}})^{1-\gamma}}{1-\gamma}=\frac{\gamma}{(1-\gamma)B_0'}. \tag{7}$$

Although standard fitting routines may be used to obtain B_0 and B_0' from a set of $(V/V_0,p)$ data, the following procedure has shown to minimize the errors associated to B_0':

(i) take an initial p_{sp};

(ii) compute the x and y vectors using Eqs. (5) and (6);

(iii) compute the least squares,

$$M_{\mathrm{opt}}=\left[\sum_i y_i(1-x_i)\right]\left[\sum_i (1-x_i)^2\right]^{-1}$$

and

$$\delta=\sum_i [y_i-M_{\mathrm{opt}}(1-x_i)]^2;$$

(iv) take a new p_{sp} and minimize the $\delta(p_{\mathrm{sp}})$ function.

B. Linear spinodal EOS

An important characteristic of the spinodal hypothesis is that the isothermal compressibility $\kappa_v(p)$ and the thermal expansion $\alpha_v(p)$ follow the same power law in the pressure:[5]

$$\kappa_v(p)=B_T(p)^{-1}=K^*[p-p_{\mathrm{ps}}]^{-\gamma}, \tag{8}$$

$$\alpha_v(p)=\alpha^*[p-p_{\mathrm{ps}}]^{-\gamma}. \tag{9}$$

If we assume that these universal relations hold for the linear compressibilities κ_a,

$$\kappa_a(p)=-\frac{1}{a}\left(\frac{\partial a}{\partial p}\right)_T=K_a^*[p-p_{\mathrm{ps}}]^{-\gamma}, \tag{10}$$

the SEOS can then be used to represent $(a/a_0,p)$ data, where a is a lattice parameter of an orthogonal (not necessarily cubic) unit cell. Using a instead of V in Eq. (5), the fitting parameter M_a is related to K_a^* and the zero-pressure linear compressibility, $\kappa_{0a}=\kappa_a(0)$, by

$$K_a^*=(1-\gamma)M_a(-p_{\mathrm{sp}})^{\gamma-1} \tag{11}$$

and

$$\kappa_{0a}=\frac{(1-\gamma)M_a}{(-p_{\mathrm{sp}})}, \tag{12}$$

where p_{sp} has been taken from the $(V/V_0,p)$ fitting. For orthogonal unit cells $\alpha=\beta=\gamma=90°$, the volumetric compressibility κ_v is related to κ_a, κ_b, and κ_c by $\kappa_v=\kappa_a+\kappa_b+\kappa_c$. Thus these systems offer a test of the consistency of the linear fitting: the relation $M_a+M_b+M_c=M$ and $K^*=K_a^*+K_b^*+K_c^*$ should hold.

The pressure derivative of the linear compressibilities is given by

$$\kappa_a' = \left(\frac{\partial \kappa_a}{\partial p}\right)_T = -\frac{\gamma K_a^*}{(p-p_{sp})^{\gamma+1}} = -\frac{\gamma \kappa_a}{(p-p_{sp})}, \quad (13)$$

with equivalent expressions for the b and c components. If we now define $B_a = 1/\kappa_a$, we obtain

$$B_a' = \frac{\gamma B_a}{[p-p_{sp}]}, \quad (14)$$

which is analogous of Eq. (3) as a function of pressure.

Finally, a direct integration of Eq. (10) gives

$$a(p) = a_{sp}\exp\left\{-\frac{K_a^*}{(1-\gamma)}[p-p_{sp}]^{1-\gamma}\right\}, \quad (15)$$

with similar expressions for $b(p)$ and $c(p)$. From the last equation, it is clear that the equilibrium volume given by Eq. (1) is exactly recovered from the cell parameters a, b, and c provided that $K^* = K_a^* + K_b^* + K_c^*$ and $V_{sp} = a_{sp} b_{sp} c_{sp}$.

C. Temperature dependence of the spinodal EOS

Recalling that the spinodal pressure depends only on T and using the Mie-Grüneisen equation,[19] Eq. (16) is readily obtained:[4,5]

$$p_{sp}(T) = p_{sp}^0 + \frac{\gamma^G}{V} E_{vib}(T), \quad (16)$$

where p_{sp}^0 is the static pseudospinodal pressure ($T=0$ K and zero-point effects neglected). Since in Eq. (16) the quotient γ^G/V is assumed to be T independent, all thermal effects are collected in $E_{vib}(T)$, the vibrational thermal energy of the solid. We have used the Einstein model to determine $E_{vib}(T)$ since, except at very low temperatures, no significant improvement is gained by using more sophisticated models such as the Debye theory.[4]

Equation (16) is the practical way to include thermal effects in the SEOS. Its use requires the determination of p_{sp}^0, once the Einstein temperature θ_E and the Grüneisen parameter γ^G are known. The static pseudospinodal pressure is computed as follows. If B_0 and B_0' are known at any reference temperature T_{ref}, they determine $p_{sp}(T_{ref})$ through Eq. (3). Then p_{sp}^0 is computed from Eq. (16). When B_0 and B_0' come from a static calculation of a set of $(V/V_0, p)$ pairs, using the fitting procedure described above, Eq. (3) gives directly p_{sp}^0. Once $p_{sp}(T)$ is available, all thermodynamic properties are obtained from the expressions derived in the previous two subsections. The zero-pressure thermal (volumetric) expansion coefficient as a function of the temperature is given by[4]

$$\alpha_{0v}(T) = \frac{1}{B_0(T)} \frac{dp_{sp}(T)}{dT}. \quad (17)$$

Analogously, thermal effects are incorporated into the linear SEOS by means of the $p_{sp}(T)$ function, and the dependence of the linear compressibilities with temperature can be evaluated. As a result, the expression for the thermal (linear) expansion coefficient for the unit-cell parameter a is

$$\alpha_a(T) = \kappa_a(T) \frac{dp_{sp}(T)}{dT}, \quad (18)$$

with equivalent expressions for $\alpha_b(T)$ and $\alpha_c(T)$. Once again, the consistency of the above equations can be checked by means of the independent evaluation of $\alpha_{0v}(T)$ using Eq. (17) and using the sum $\alpha_{0a}(T) + \alpha_{0b}(T) + \alpha_{0c}(T)$, which has to be fulfilled in orthogonal lattices.

III. RESULTS AND DISCUSSION

A. SEOS description of isothermal theoretical and experimental data

The fitting procedure has been applied to (V,p), (a,p), and (c,p) pairs in rutile TiO_2 using theoretical and experimental data. The theoretical values have been obtained from *ab initio* perturbed ion calculations. This model is a localized Hartree-Fock scheme appropriate for the description of structural and mechanical properties of ionic materials (see Refs. 20, 21, and references therein). By minimizing the Gibbs energy of the crystal at static conditions, we generate data for the volume and lattice parameters a and c as pressure is applied (see Ref. 22 for details). In the minimizations, the internal parameter x of the unit cell has been fixed at the experimental value of 0.3048.[23] For the sake of completeness, we have carried out calculations releasing this constraint. We have found that this freedom does not significantly modify the energy-volume curve: at zero pressure the optimum x value is found to be only 3% higher than the experimental value. For other computational information, we refer to our recent work on the anatase phase of TiO_2.[24]

Furthermore, we have used two sets of experimental data: One set contains the isothermal compression data from Ming and Manghnani obtained in x-ray-diffraction experiments on a polycrystalline sample of TiO_2.[15] In that work, there is detailed information (with 18 points) of pressure effects on V, a, and c up to 10.6 GPa. The second set contains the recent results obtained by Gerward *et al.*[13] from x-ray powder-diffraction measurements performed in high-pressure anvil cells at room temperature: 7 points for the volume and 12 points for the lattice parameters in the ranges 0–7.97 and 0–14 GPa, respectively. Fitting the Birch-Murnaghan EOS to these data without fixing B_0' gives $B_0 = 210 \pm 10$ GPa and $B_0' = 6.6 \pm 0.7$.

Results of these fittings are presented in Figs. 1 and 2. In these plots, f refers to either V, a, or c, and f_0 to their corresponding zero-pressure values. It is apparent that the observed and simulated behavior of the three variables follow accurately the spinodal conduct. The root-mean-square deviations of the fittings can be transferred to uncertainties in the input f values. We have found that these uncertainties are less than 0.3% and 0.1% in the experimental and theoretical fittings, respectively.

We should note that a direct comparison between the corresponding theoretical and experimental SEOS curves is not

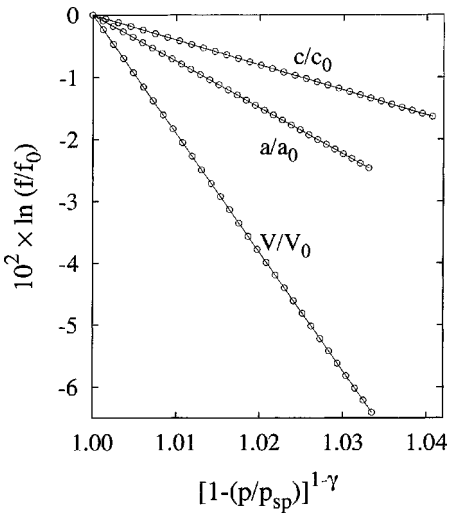

FIG. 1. Spinodal fitting to theoretical data. Empty circles (○) represent the *aiPI* values and solid lines the fitting functions [Eq. 5)].

possible since the abscissa of Figs. 1 and 2 contains the spinodal pressure, which depends on the source of the input data. The complete set of spinodal parameters resulting from the $p-V$ fittings are collected in Table I. In order to check the suitability of the fitting procedure described in Sec. II A, we have used a standard Levengerg-Marquard routine to fit the SEOS to the (unweighted) experimental data. The resulting parameters are $B_0=211\pm9$ GPa and $B_0'=6.8\pm2.6$, in excellent agreement with the results from Table I. The experimental spinodal curve yields a global good agreement with preexistent data. The value derived for B_0 from this curve when both the Ming and Manghnani[15] and Gerward and co-workers[13] data are used in the fitting (210.7 GPa) agrees very well with the value reported in Ref. 7 (211.3 GPa) and with the value derived by Ming and Manghnani[15]

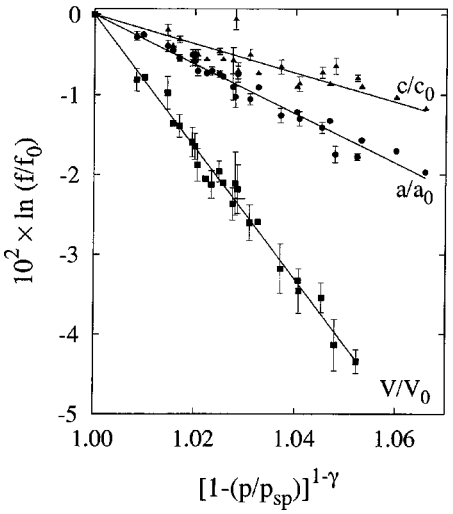

FIG. 2. Spinodal fitting to experimental data. Symbols represent the experimental data of Ming and Manghnani (Ref. 15) (with error bars) and Gerward *et al.* (Ref. 13) (without error bars). Solid lines represent the fitting functions [Eq. (5)].

from their Birch-Murnaghan fitting (211 ± 7 GPa). The values of B_0' from the two fittings show some discrepancy: $B_0'=5.88$ when the data from Ming and Manghnani[15] are used, but $B_0'=6.83$ if the two sets of data are included. A lower value for B_0' is found from the theoretical spinodal EOS. Since the agreement in B_0 is very good, Eq. (3) clearly establishes that the difference between experimental and theoretical spinodal values for B_0' is due to the differences in the corresponding spinodal pressures.

To analyze further the difference between experimental and theoretical spinodal values for B_0', we have recovered the energy-volume ($E-V$) curves by integrating the experimental and theoretical spinodal equations. The results are depicted in Fig. 3. It can be seen that, in spite of the good agreement between the two curves around the equilibrium geometry and in the left branches of positive pressures, there is a clear deviation from each other as V deviates from V_0. This deviation induces the change of curvature, which defines the spinodal pressure, to occur first in the experimental spinodal energy-volume curve, as expected. It is clear from Eq. (3) that in order to produce B_0' values in good agreement with experiment, a theoretical method must be able to determine very accurately this change of curvature. In conclusion, all these aspects indicate the great sensibility of the SEOS to different B_0 and B_0' parameters.

Now, we proceed to the analysis of the behavior of the unit-cell parameters under pressure. The observed and calculated lower compressibility of the *c* axis with respect to the *a* one is a consequence of the alignment of the TiO_6 edge-sharing octahedra along the *c* axis. These data are well described by our proposed linear SEOS. First, it is interesting to compare the values of the $K^\star$, M, and V_{sp} parameters derived from the $(V/V_0,p)$ fitting with those obtained from the two linear fittings, i.e., $K^\star=2K_a^\star+K_c^\star$, $M=2M_a+M_c$, and $V_{sp}=\frac{1}{2}a_{sp}^2c_{sp}$ (the factor $\frac{1}{2}$ is necessary to account for the two molecular formulas in the unit cell of rutile, as V_{sp} stands for the molecular volume). As it is evident from the results of Table I, this test is accurately satisfied when the experimental set of data is exclusively that of Ming and Manghnani.[15] When the Gerward and co-workers[13] experimental measurements are also included in the SEOS fitting, the agreement is not perfect but is still reasonably good. The theoretical values of these three parameters are also approximately recovered from their linear analogues. Second, the theoretical and experimental spinodal κ_{0a} and κ_{0c} parameters are consistent with each other and consistent also with the value for the bulk compressibility (κ_{0v}) derived from the spinodal fittings to the $p-V$ data. Our values are somewhat greater than those proposed by Ming and Manghnani after simple linear fittings[15] ($\kappa_{0a}=16.4\times10^{-4}$ GPa^{-1}, $\kappa_{0c}=9.1\times10^{-4}$ GPa^{-1}). We should notice in this respect that their value for κ_{0v} (41.9×10^{-4} GPa^{-1}) derived from κ_{0a} and κ_{0c} is more than 10% lower than the one directly obtained from the $p-V$ Birch-Murnaghan fitting.

The linear SEOS can also be checked using the c/a ratio. The Taylor expansion of Eq. (15) around $p=0$ gives the relation

TABLE I. Parameters for rutile TiO_2 derived from the fitting to the spinodal EOS of the experimental and (static) theoretical $(V/V_0,p)$ data.

	SEOS theor.	SEOS expt. [a]	SEOS expt. [b]
B_0 (GPa)	212.8	213.8	210.7
B_0'	2.96	5.88	6.83
B_0'' (GPa^{-1})	−0.007	−0.029	−0.039
$-p_{sp}^0$ (GPa)	61.13	33.17	28.50
$K^\star$ ($GPa^{\gamma-1}$)	0.155, 0.160 [c]	0.086, 0.086 [c]	0.076, 0.073 [c]
M	1.915, 1.960 [d]	0.963, 0.963 [d]	0.829, 0.800 [d]
V_{sp}	1407, 1487 [e]	552, 552 [e]	481, 469 [e]
V_0 ($bohr^3$/molec)	207.15 [f]	211.16 [g]	211.16 [g]
κ_{0v} (10^4 GPa^{-1})	48.48, 49.61 [h]	46.77, 46.77 [h]	47.45, 45.84 [h]
κ_{0a} (10^4 GPa^{-1})	18.61	18.45	17.70
κ_{0c} (10^4 GPa^{-1})	12.40	9.87	10.43

[a]Experimental data only from Ming and Manghnani (Ref. 15).
[b]Experimental data from Ming and Manghnani (Ref. 15) and Gerward and co-workers (Ref. 13).
[c]$K^\star = 2K_a^\star + K_c^\star$.
[d]$M = 2M_a + M_c$.
[e]$V_{sp} = \frac{1}{2} a_{sp}^2 c_{sp}$.
[f]Static *aiPI* calculation.
[g]Experimental value from Isaak *et al.* (Ref. 7).
[h]$\kappa_{0v} = 2\kappa_{0a} + \kappa_{0c}$.

$$c(p,T)/a(p,T) = t_0 + t_1 \times p,$$

where

$$t_0 = \frac{c_{sp}}{a_{sp}} \exp\left[-\frac{(K_c^\star - K_a^\star)}{1-\gamma} (-p_{sp})^{1-\gamma} \right]$$

and

$$t_1 = -t_0 \times (K_c^\star - K_a^\star)(-p_{sp})^{-\gamma}.$$

Fitting this expression to the Ming and Manghnani experimental data yields $t_0 = 0.645\,17$ and $t_1 = 0.055\,36 \times 10^{-2}$ GPa^{-1}, in very good agreement with the parameters of these authors ($t_0 = 0.645$ and $t_1 = 0.056 \times 10^{-2}$ GPa^{-1}).

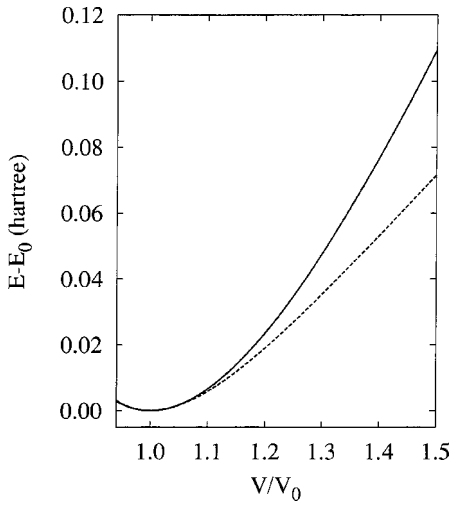

FIG. 3. Integrated experimental (dashed line) and theoretical (solid line) spinodal equations of state.

All these results reveal that Eq. (15) proposed in this work gives a very accurate description of the pressure response of the cell parameters of rutile TiO_2.

B. SEOS description of thermal effects

In this section, we make use of the temperature-dependent SEOS [Eq. (16)] in two different situations. In the first one, thermal effects are incorporated in our static theoretical results with the aim of comparing them with the experimental data at room temperature. In the second one, we evaluate the behavior of rutile TiO_2 as temperature increases using the experimental room-temperature information as the reference data in the SEOS.

A practical use of Eq. (16) needs some input values for γ^G and θ_E parameters (see Table II). We have proceed in two different ways according to the two cases explained above. As far as computation of thermal effects on the static calculations is concerned, these two parameters have been estimated from the static *aiPI* (V,p) values by means of the quasi-harmonic Debye model of Ref. 22. Using p_{sp}^0 from the theoretical SEOS (Table I), we obtain $p_{sp}(300\ K)$ and calculate new theoretical curves for $V(p)$, $a(p)$, and $c(p)$ at 300 K. In Fig. 4, we can observe a good agreement with the experimental data of Ming and Manghnani[15] and Gerward and co-workers.[13] In particular, $V_0(300)$ obtained through the thermal SEOS increases to 209.33 $bohr^3$/mol from 207.15 $bohr^3$/mol at static conditions, approaching the room temperature experimental value (210.59–211.16 $bohr^3$/mol). Our theoretical estimation for α_{0v} at ambient conditions is also in reasonable agreement with the experimental data. In addition, the calculated linear SEOS at 300 K produces linear thermal expansions (α_a and α_c) that recover quite well the volumetric behavior (see Table II).

TABLE II. Zero pressure bulk and linear properties of rutile TiO_2 at $T=300$ K.

	SEOS theor.	SEOS expt. [a]	SEOS expt. [b]	Expt.
$\gamma^G(V_0)$	1.36 [c]	1.50 [d]	1.50 [d]	
$\theta_E=0.75\theta_D$ (K)	620 [c]	567 [e]	567 [e]	
$T_{\rm ref}$ (K)	static	300	300	
V_0 (bohr^3/mol)	209.33	211.16	211.16	210.59, [f] 211.16 [g]
a (bohr)	8.3939	8.6746	8.6746	8.6746 [f]
c (bohr)	6.0061	5.5966	5.5966	5.5966 [f]
α_{0v} (10^6 K^{-1})	18.85, 19.29 [h]	20.90, 20.91 [h]	21.21, 20.49 [h]	23.52, [i] 22.5, [j] 16.1 [k]
α_{0a} (10^6 K^{-1})	7.23	8.25	7.91	
α_{0c} (10^6 K^{-1})	4.82	4.41	4.66	

[a]Experimental data only from Ming and Manghnani (Ref. 15).
[b]Experimental data from Ming and Manghnani (Ref. 15) and Gerward co-workers (Ref. 13).
[c]Value obtained from the *aiPI* (V,p) data using the quasiharmonic Debye model of Ref. 22.
[d]Average value of Ref. 7 over the whole range of temperature (300–1800 K).
[e]Value computed in this work from the room-temperature isothermal elastic constants of Ref. 7 by solving the Christoffel equations of the crystal (Ref. 25).
[f]Reference 15.
[g]Reference 7.
[h]$\alpha_{0v}=2\alpha_{0a}+\alpha_{0c}$.
[i]Reference 26.
[j]Reference 16.
[k]Reference 17.

Concerning the second application of the thermal SEOS, we have evaluated $p_{\rm sp}^0$ using the $p_{\rm sp}$(300-K) experimental SEOS. Here, γ^G has been obtained as the average value of the reported γ^G values in Ref. 7 over the whole range of temperatures (300–1800 K). On the other hand, θ_E has been calculated after solving the Christofell equations of the crystal[25] using the room-temperature isothermal elastic constants obtained by Isaak *et al.*[7] The study of thermal effects on rutile TiO_2 has been performed in the range 0–2000 K. The temperature dependence of V_0, B_0, and α_{0v} is displayed in Figs. 5–7, respectively, along with the experimental data obtained by Toulokian *et al.*[16] and Saxena *et al.*[17] (collected by Isaak *et al.*[7]).

It is clear from Fig. 5 that the predictions derived from the SEOS, either experimental or theoretical, reproduce success-

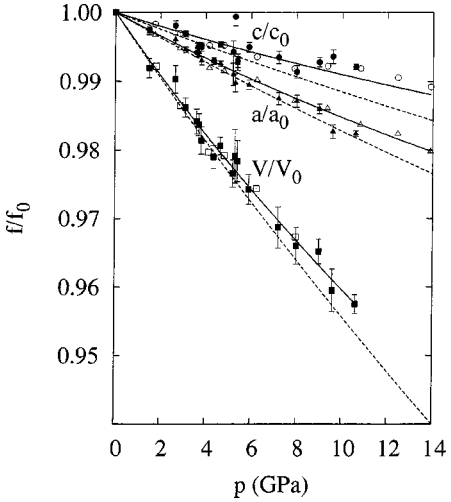

FIG. 4. Room-temperature ($T_{\rm ref}=300$ K) spinodal equation of state for experimental and theoretical data. Bold and empty symbols are the experimental data of Ming and Manghnani (Ref. 15) and Gerward *et al.* (Ref. 13), respectively. Solid lines represent the experimental SEOS fittings. Dashed lines were calculated from the theoretical SEOS fittings.

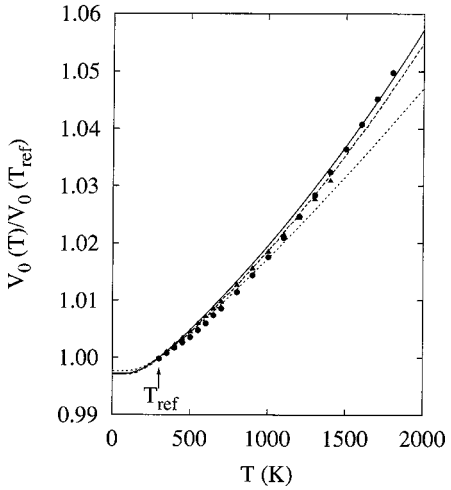

FIG. 5. Molecular volume of rutile TiO_2 at zero pressure as a function of temperature. Triangles and circles represent the experimental data of Touloukian *et al.* (Ref. 16) and Saxena *et al.* (Ref. 17). The solid line is the thermal SEOS calculated from the (V/V_0-p) experimental data at $T_{\rm ref}=300$ K; the dashed line represents the prediction of the molecular volume from the thermal linear SEOS calculated from the (a/a_0-p) and (c/c_0-p) data at $T_{\rm ref}=300$ K; the dotted line is the thermal SEOS calculated from the theoretical *aiPI* (V/V_0-p) data.

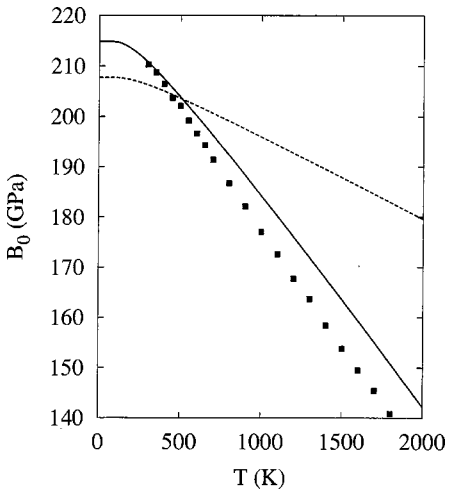

FIG. 6. Zero-pressure bulk modulus of rutile as a function of temperature. Symbols represent the experimental data of Saxena *et al.* (Ref. 17). The solid line is the thermal SEOS calculated from the (V/V_0-p) experimental data at $T_{\mathrm{ref}}=300$ K; the dashed line is the thermal SEOS calculated from the theoretical $aiPI$ (V/V_0-p) data.

fully the thermal expansion of rutile. As regards the behavior of $B_0(T)$ and $\alpha_{0v}(T)$ (Figs. 6 and 7), the divergence between the experimental data and the SEOS is greater than in the case of $V_0(T)$. Nevertheless, although only the equilibrium volume and the γ^G and θ_E parameters at T_{ref} are required, the experimental SEOS provides a global satisfactory description of these properties. The largest deviation with respect to the experimental values of B_0 is observed at the highest temperature, and is lower than 10 GPa. With respect to α_{0v}, the experimental SEOS curve lies between the two sets of experimental data in the high-temperature range. Besides, it is also to be noticed that the results obtained with the linear form are highly consistent with those of the standard SEOS. The discrepancies between the theoretical and the experimental SEOS are again due to the different values of the spinodal pressures.

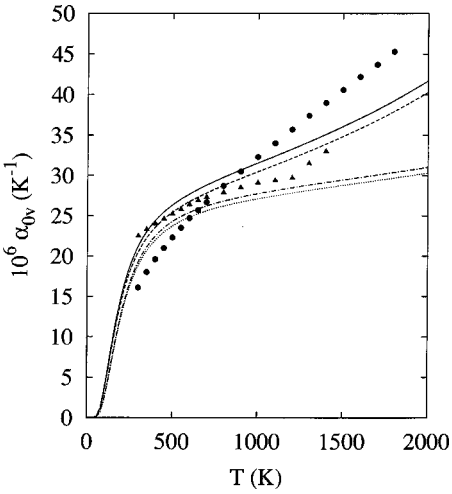

FIG. 7. Zero pressure volumetric thermal-expansion coefficient of rutile as a function of temperature. Triangles and circles represent the experimental data of Touloukian *et al.* (Ref. 16) and Saxena *et al.* (Ref. 17). The solid line is the thermal SEOS calculated from the (V/V_0-p) experimental data at $T_{\mathrm{ref}}=300$ K; the dashed line represents the predictions from the thermal linear SEOS calculated from the (a/a_0-p) and (c/c_0-p) data at $T_{\mathrm{ref}}=300$ K; the dotted line is the thermal SEOS calculated from the theoretical $aiPI$ (V/V_0-p) data; the dashed-dotted line represents the predictions from the thermal linear SEOS calculated from the $aiPI$ (a/a_0-p) and (c/c_0-p) data.

A final issue that deserves some discussion is related to the comparison of the effects of pressure and temperature on the unit-cell parameters. Contrarily to the observed behavior, our predictions for the linear-expansion coefficients (see Table II) reveal a dilatation along the *a* axis greater than that along the *c* axis as *T* increases. Since the thermal SEOS has been derived from the $p-V$ behavior at a reference temperature, the behavior of the solid when *T* increases can be understood as an extrapolation to negative pressures of the rutile response to hydrostatic pressure. This is in fact the behavior found in many solids that follow the so-called inverse relationship guided by the molecular volume. Hazen and Finger[18] have shown that the c/a ratio increases in rutile with temperature, breaking the inverse relationship since this ratio also increases as pressure is applied. For this particular situation, the law of corresponding states does not work properly and at least two reference states at different temperatures are needed.

IV. CONCLUSIONS

In this work, we present a general strategy to describe $p-T-V$ and $p-T-$ lattice parameter data using the spinodal equation of state. As concerns the isothermal behavior, the EOS parameters are obtained by means of a fitting procedure that involves root-mean-square linear minimizations in each step. To evaluate the thermodynamic properties of a solid at different temperatures using the spinodal scheme, we have shown that only the spinodal pressure at a reference temperature, the Einstein temperature θ_E and the Grüneisen parameter γ^G are needed.

For rutile TiO_2, we can accurately describe with this function the pressure dependence of theoretical (static) and two sets of experimental (room-temperature) volume and lattice parameter values. The numerical procedure shows a great sensibility of B_0' to the input data. Our most complete fitting yields $B_0=210.7$ GPa and $B_0'=6.83$, in very good agreement with preexistent experimental values. The proposed linear SEOS has proved to be a stable function with linear compressibilities that recover the bulk behavior. As expected, κ_{0c} is found to be lower than κ_{0a}, our values being slightly higher than those previously reported by Ming and Manghnani.[15]

The $aiPI$ static calculations have been corrected to account for the thermal effects using the SEOS strategy. At 300 K, the theoretical prediction of the rutile unit-cell response to hydrostatic pressure is in agreement with the experimental behavior. In addition, the zero pressure α_{0v}, α_{0a}, and α_{0c} coefficients derived from the theoretical and experimental

SEOS show small differences. We have also evaluated the thermodynamic properties of rutile in the range 0–2000 K using the zero pressure experimental data at 300 K. Our results reveal that the SEOS produces a very good description of the solid at high temperature in terms of the molecular volume, the bulk modulus, and the volumetric thermal-expansion coefficient. Failure to predict the behavior of the c/a ratio at increasing temperature is explained as due to the breakdown of the inverse relationship observed in the rutile structure of TiO_2.

ACKNOWLEDGMENTS

Financial support from the DGICYT, Project Nos. BQU2000-0466 and PB98-0832, is hereby acknowledged. L.G. is grateful for financial support from the Danish Natural Sciences Research Council through DANSYNC.

[1] See, for example, G.J. Ackland, Rep. Prog. Phys. **64**, 483 (2001), and references therein.

[2] V. García Baonza, M. Cáceres, and J. Nuñez, Phys. Rev. B **51**, 28 (1995).

[3] M. Taravillo, V. García Baonza, J.E.F. Rubio, J. Nuñez, and M. Cáceres, J. Phys. Chem. Solids **63**, 1705 (2002).

[4] V. García Baonza, M. Taravillo, M. Cáceres, and J. Nuñez, Phys. Rev. B **53**, 5252 (1996).

[5] M. Taravillo, V. García Baonza, J. Nuñez, and M. Cáceres, Phys. Rev. B **54**, 7034 (1996).

[6] P. Vinet, J.R. Smith, J. Ferrante, and J.H. Rose, Phys. Rev. B **35**, 1945 (1987).

[7] D.G. Isaak, J.D. Carnes, O.L. Anderson, H. Cynn, and E. Hake, Phys. Chem. Miner. **26**, 31 (1998).

[8] M. Mikami, S. Nakamura, O. Kitao, H. Arakawa, and X. Gonze, Jpn. J. Appl. Phys., Part 2 **39**, L847 (2000).

[9] A.C. Camargo, J.A. Igualada, A. Beltrán, R. Llusar, E. Longo, and J. Andrés, Chem. Phys. **212**, 381 (1996).

[10] J.K. Dewhurst and J.E. Lowther, Phys. Rev. B **54**, R3673 (1996).

[11] S.D. Mo and W.Y. Ching, Phys. Rev. B **51**, 13 023 (1995).

[12] K.M. Glassford and J.R. Chelikowsky, Phys. Rev. B **46**, 1284 (1992).

[13] L. Gerward and J. Staun Olsen, J. Appl. Crystallogr. **30**, 259 (1997); J. Staun Olsen, L. Gerward, and J.Z. Jiang, J. Phys. Chem. Solids **69**, 229 (1999).

[14] J. Haines and J.M. Léger, Physica B **192**, 233 (1993).

[15] L. Ming and M.H. Manghnani, J. Geophys. Res. **84**, 4777 (1979).

[16] Y. S. Touloukian, R. K. Kirby, R. E. Taylor, and T. Y. R. Lee, in *Thermophysical Properties of Matter* (IFI/Plenum, New York, Washington, 1977), Vol. 13.

[17] S. K. Saxena, N. Chatterjee, Y. Fei, and G. Shen, *Thermodynamic Data on Oxides and Silicates: An Assessed Data Set Based on Thermochemistry and High-Pressure Phase Equilibrium* (Springer-Verlag, Berlin, 1993).

[18] R.M. Hazen and L.W. Finger, J. Phys. Chem. Solids **42**, 143 (1981).

[19] M. Ross and D.A. Young, Annu. Rev. Phys. Chem. **44**, 61 (1993).

[20] V. Luaña and L. Pueyo, Phys. Rev. B **41**, 3800 (1990).

[21] V. Luaña, A. Martín Pendás, J.M. Recio, E. Francisco, and M. Bermejo, Comput. Phys. Commun. **77**, 107 (1993); M.A. Blanco, V. Luaña, and A. Martín Pendás, *ibid.* **103**, 287 (1997).

[22] E. Francisco, M.A. Blanco, and G. Sanjurjo, Phys. Rev. B **63**, 094107 (2001).

[23] S.C. Abrahams and J.L. Bernstein, J. Chem. Phys. **55**, 3206 (1971).

[24] T. Arlt, M. Bermejo, M.A. Blanco, L. Gerward, J.Z. Jiang, J. Staun Olsen, and J.M. Recio, Phys. Rev. B **61**, 14 414 (2000).

[25] R.A. Robie and J.L. Edwards, J. Chem. Phys. **37**, 2659 (1966).

[26] R.K. Kirby, J. Res. Natl. Bur. Stand., Sect. A **71A**, 363 (1967).